

# Garbage Attention in Large Language Models: <BOS> Sink Heads and Sink-aware Pruning

Jaewon Sok<sup>2</sup> Jewon Yeom<sup>1</sup> Seonghyeon Park<sup>3</sup> Jeongjae Park<sup>1</sup> Taesup Kim<sup>1,\*</sup>

<sup>1</sup>Graduate School of Data Science, Seoul National University

<sup>2</sup>Department of Rural Systems Engineering, Seoul National University

<sup>3</sup>Department of Aerospace Engineering, Seoul National University

## Abstract

Large Language Models (LLMs) are known to contain significant redundancy, yet a systematic explanation for why certain components, particularly in higher layers, are more redundant has remained elusive. In this work, we identify the <BOS> sink phenomenon as a key mechanism driving this layer-wise sensitivity. We show that attention heads with high <BOS> sink scores are strongly associated with functional redundancy: such heads, especially in deeper layers, contribute little to predictive performance and effectively serve as *dumping grounds* for superfluous attention weights. This provides a concrete functional explanation for the structural redundancy reported in prior studies. Leveraging this insight, we introduce a simple pruning strategy that removes high-<BOS> sink heads. Experiments on Gemma-3, Llama-3.1, and Qwen3 demonstrate that this approach identifies redundant transformer components more reliably than weight- or activation-based criteria, while preserving performance close to dense baselines even under aggressive pruning. Moreover, we find that the behavior of sink heads remains stable across different sequence lengths. Overall, our results suggest that structural properties of attention offer a more intuitive and robust basis for model compression than magnitude-based methods.

## 1 Introduction

The advent of Transformers (Vaswani et al., 2017) has enabled Large Language Models (LLMs) to achieve unprecedented performance on various tasks (Brown et al., 2020; Zhao et al., 2023). However, the massive parameter spaces of these models contain significant redundancy (Michel et al., 2019; Fan et al., 2025; He et al., 2024; Kaushik et al., 2025), serving as a primary bottleneck for efficient deployment. Consequently, while much effort has

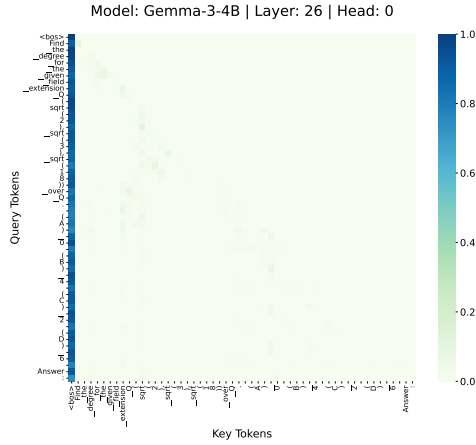


Figure 1: Attention weights of a representative <BOS> sink head (L26, H0) in Gemma-3-4B. The heatmap reveals a stark attention sink pattern where query tokens disproportionately attend to the <BOS> token during an MMLU task.

been devoted to model compression and pruning (Hoefer et al., 2021; Zhu et al., 2024; Song et al., 2024), the underlying nature and origins of this redundancy remain relatively unexplored.

Previous research on the attention mechanism, the cornerstone of the Transformer architecture, has demonstrated that individual attention heads perform distinct functional roles (Clark et al., 2019b; Voita et al., 2019). Notably, a phenomenon known as the *attention sink* has been identified, where attention weights are disproportionately concentrated on specific tokens, particularly the Beginning-of-Sentence (<BOS>) token (Xiao et al., 2024). Further analysis reveals that this behavior is driven by specialized attention heads that exhibit a remarkably high propensity for such effects (Queipo-de Llano et al., 2025). The importance of attention sinks is evidenced by the substantial performance degradation observed when omitting the <BOS> token at inference time in models trained with it (Barbero et al., 2025).

In parallel, structural pruning studies have in-

\* Corresponding author.

creasingly focused on the layer-wise sensitivity of LLMs to identify redundant components. A recurring observation in this line of work is that LLMs exhibit a non-uniform distribution of importance across their depth, with higher layers often being more amenable to pruning or skipping without catastrophic performance loss (Gromov et al., 2025; Zhang et al., 2024; Men et al., 2025). Recent studies further demonstrate that attention heads in higher layers can be effectively pruned, particularly when combined with rescaling to preserve representation stability (Liu and Liu, 2025).

Despite their importance in training, the functional role in inference of attention sink heads remains largely underexplored. Moreover, while prior pruning literature consistently reports the redundancy of higher layers, the criteria for defining these layers have not yet been systematically established, and the underlying reasons are often limited to post-hoc explanations.

In this work, we make the following contributions:

- We identify  $\langle \text{BOS} \rangle$  sink heads (Figure 1) as structurally specialized attention heads that act as *dumping grounds* for superfluous attention weights, providing a mechanistic explanation for redundancy in LLMs.
- We show that the emergence and concentration of these heads in higher layers explains the layer-wise sensitivity consistently observed in prior pruning literature.
- We demonstrate that  $\langle \text{BOS} \rangle$  sink scores constitute a simple yet robust structural metric for identifying redundant heads and layers, enabling effective structured pruning while preserving predictive performance.

## 2 Related Work

### 2.1 Attention Sink

The attention sink phenomenon refers to the observation that LLMs consistently allocate disproportionate attention weights to initial tokens, particularly the  $\langle \text{BOS} \rangle$  token, regardless of their semantic relevance. Xiao et al. (2024) first identified this behavior, attributing it to the softmax operation’s requirement for attention scores to sum to one, which leads the model to use the first token as a *sink* to *dump* unnecessary attention weights.

Gu et al. (2025) demonstrated that attention sinks are not innate, but gradually emerge during the

pre-training phase as a learned strategy for managing attention distribution. Furthermore, Queipo-de Llano et al. (2025) established that this behavior is driven by specialized *sink heads* and is intrinsically linked to *compression valleys*, specific regions in the model that exhibit both high attention sink activity and high redundancy. Their analysis revealed that these sink heads effectively act as functional “no-ops”.

The functional necessity of maintaining these sinks is underscored by their impact on model stability. Barbero et al. (2025) found that for models specifically trained to utilize the  $\langle \text{BOS} \rangle$  token as an attention sink, omitting it at inference time leads to significantly degraded performance. Collectively, these findings suggest that while attention sinks represent a form of redundancy, the  $\langle \text{BOS} \rangle$  token itself plays a vital structural role as a stable anchor for the model’s internal representations.

Building on this tension between structural necessity and functional redundancy, we investigate whether these specialized sink heads can be selectively removed from pre-trained LLMs. Given their role as repositories for unnecessary attention weights, effectively acting as *dumping grounds*, we explore the potential for inference-time pruning of these heads to enhance model efficiency without catastrophic degradation of performance.

### 2.2 Pruning Methods

Pruning mitigates overhead in LLMs by eliminating redundant parameters. While unstructured pruning targets individual weights (Sun et al., 2024; Frantar and Alistarh, 2023), structured approaches remove entire architectural units—such as attention heads or layers—to ensure direct hardware compatibility and immediate inference speedups (Ma et al., 2023; Ashkboos et al., 2024; Men et al., 2025; Yang et al., 2024). Depending on the target unit, structured pruning is typically categorized into component-level and layer-level pruning.

**Unstructured Pruning** This fine-grained approach aims for high sparsity while maintaining performance. Foundational Magnitude Pruning (Han et al., 2015) assumes that weights with smaller absolute values possess lower functional importance. To enhance static analysis, Wanda (Sun et al., 2024) and Wanda++ (Yang et al., 2025c) incorporate input activation norms and regional gradients, respectively. Furthermore, SparseGPT (Frantar and Alistarh, 2023) enables one-shot com-

pression of massive models by solving a large-scale weight reconstruction problem.

**Component-level Pruning** Research in this area identifies redundant sub-structures while addressing architectural dependencies. LLM-Pruner (Ma et al., 2023) represents an early effort using gradient-based saliency to prune non-critical coupled structures. Subsequently, FLAP (An et al., 2024) introduced a novel fluctuation-based importance metric and extended established principles (Han et al., 2015; Sun et al., 2024), such as magnitude-based (Mag-SP) and activation-scaled (Wanda-SP) metrics, to the requirements of structured pruning. Diverging from saliency-based methods, SliceGPT (Ashkboos et al., 2024) leverages computational invariance to reduce model width by deleting entire rows and columns.

**Layer-level Pruning** To achieve maximum efficiency, recent studies target the removal of entire transformer blocks. A representative approach is ShortGPT (Men et al., 2025), which quantifies layer redundancy through the Block Influence (BI) metric, measuring the cosine similarity of representation transformations. Similarly, LaCo (Yang et al., 2024) proposes layer collapse to merge blocks, while methods like SLEB (Song et al., 2024) and EntroDrop (Yang et al., 2025b) refine selection through similarity analysis or information richness metrics.

### 3 Preliminary

#### 3.1 Attention Sink Metrics

To analyze how attention is allocated across different tokens, we adopt the metrics from Gu et al. (2025). Let  $\alpha_{t,k}^{(\ell,h)}$  denote the attention weight from the query token at position  $t$  to the key token at position  $k$  in the  $h$ -th head of the  $\ell$ -th layer.

**Attention Sink Score** First, we utilize the attention sink score to quantify the degree to which a specific token position  $k$  attracts attention weights within a head. For a sequence of length  $T$ , the score for token  $k$  in head  $h$  of layer  $\ell$  is defined as the average attention weight it receives from all tokens in the sequence:

$$\text{sink-score}_k^{(\ell,h)} = \frac{1}{T} \sum_{t=0}^{T-1} \alpha_{t,k}^{(\ell,h)}. \quad (1)$$

A high score indicates that the token at position  $k$  serves as a primary destination for attention

weights within that specific head.

**<BOS> Sink Score** Given that the <BOS> token (at index  $k = 0$ ) often acts as a focal point for attention, we define the <BOS> sink score to measure its influence at both the head and layer levels. The head-wise <BOS> sink score  $S_{<\text{BOS}>}^{(\ell,h)}$  and the layer-wise <BOS> sink score  $S_{<\text{BOS}>}^{(\ell)}$  are defined as follows:

$$\begin{aligned} S_{<\text{BOS}>}^{(\ell,h)} &= \text{sink-score}_0^{(\ell,h)}, \\ S_{<\text{BOS}>}^{(\ell)} &= \frac{1}{H} \sum_{h=1}^H S_{<\text{BOS}>}^{(\ell,h)}, \end{aligned} \quad (2)$$

where  $H$  is the total number of attention heads in layer  $\ell$ . The layer-wise <BOS> sink score  $S_{<\text{BOS}>}^{(\ell)}$  serves as an aggregate metric to evaluate the dependence of layer  $\ell$  on the <BOS> token.

#### 3.2 Block Influence Score

To identify redundant layers within LLMs, Men et al. (2025) leverages the Block Influence (BI) score within the ShortGPT method. This metric quantifies the degree of representation transformation performed by each layer by measuring the distance between its input and output hidden states.

**Definition** Let  $X_{i,t} \in \mathbb{R}^d$  denote the  $t$ -th row of the hidden state matrix (corresponding to the  $t$ -th token) at the  $i$ -th layer. The BI score for the  $i$ -th layer is defined as:

$$\text{BI}_i = 1 - \mathbb{E}_{X,t} \frac{X_{i,t}^T X_{i+1,t}}{\|X_{i,t}\|_2 \|X_{i+1,t}\|_2}, \quad (3)$$

where  $\|\cdot\|_2$  denotes the  $L_2$  norm, and the expectation  $\mathbb{E}_{X,t}$  is taken over a dataset  $X$  and token positions  $t$ .

### 4 <BOS> Sink as a Marker of Functional Redundancy

**<BOS> Sink Score Extraction** To analyze the model’s internal behavior, we calculate the <BOS> sink score defined in Equation 2. Specifically, we perform zero-shot inference on the MMLU dataset and extract attention weights directly from the attention maps during the initial decoding step.

**Head-wise Ablation** Figure 2 illustrates the impact of individual head ablation on MMLU accuracy relative to <BOS> sink scores across the evaluated models. A shared characteristic among Llama-3.1-8B, Qwen3-4B, and Gemma-3-4B is

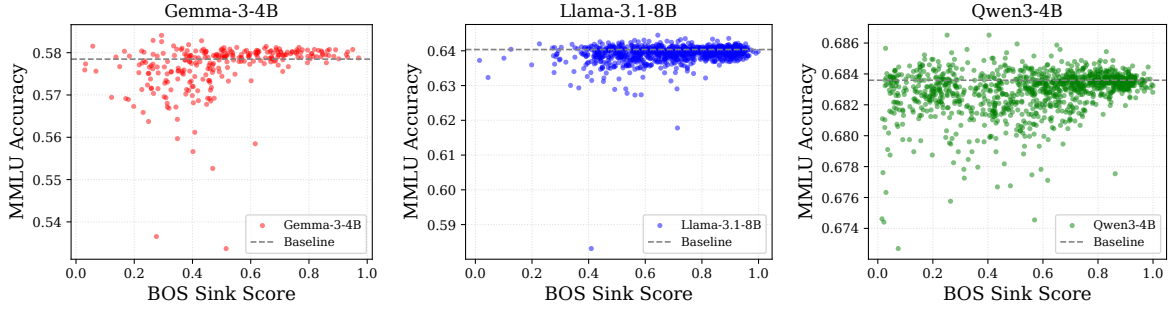


Figure 2: Impact of single-head ablation on MMLU accuracy relative to  $\langle \text{BOS} \rangle$  Sink Scores across Gemma-3-4B, Llama-3.1-8B and Qwen3-4B. Each dot represents an individual attention head, while the horizontal dashed line indicates the baseline MMLU accuracy for each respective model. A consistent pattern emerges across all three architectures: heads with high  $\langle \text{BOS} \rangle$  Sink Scores exhibit negligible impact on model performance when ablated.

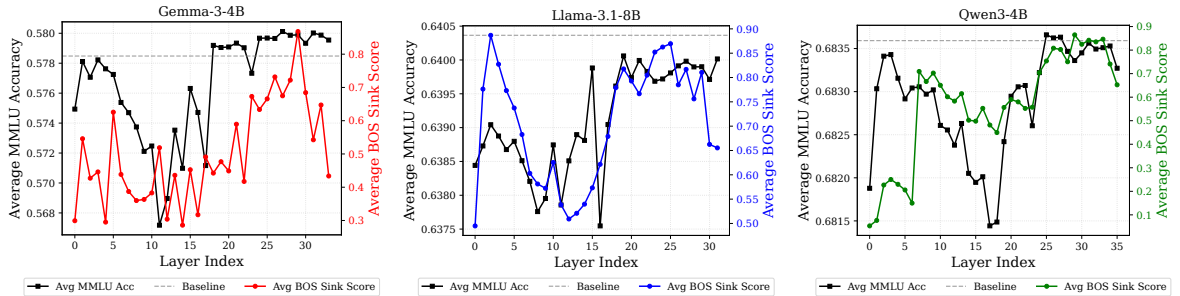


Figure 3: Correlation between  $\langle \text{BOS} \rangle$  sink scores and head ablation impact on MMLU accuracy. Colored and black lines represent layer-average sink scores (right axis) and mean MMLU accuracy under single-head ablation (left axis), respectively. In deeper layers, high sink scores strongly correlate with minimal functional necessity, indicating head redundancy.

the distinct bifurcation of performance sensitivity between low and high BOS score regimes.

In the high  $\langle \text{BOS} \rangle$  sink score regime, all three models exhibit remarkable stability. Removing these heads results in negligible performance degradation, with accuracy remaining consistently near the dense baseline. This suggests that heads exhibiting intense  $\langle \text{BOS} \rangle$  sink behavior are largely redundant for downstream task inference, regardless of the model’s architecture.

Conversely, the lower  $\langle \text{BOS} \rangle$  score regime is characterized by heightened sensitivity and increased performance fluctuations across all models. While this instability is observable in all tested architectures, it is particularly pronounced in Gemma-3-4B. Whereas Llama-3.1-8B and Qwen3-4B maintain a relatively dense clustering of performance points near their respective baselines despite occasional outliers, Gemma-3-4B exhibits a much wider dispersion and a consistent downward shift in MMLU accuracy. We hypothesize that this systemic vulnerability is tied to its leaner head architecture; specifically, Gemma-3-4B’s use of only

272 total heads, significantly fewer than the 1,024 and 1,152 heads in Llama-3.1-8B and Qwen3-4B, respectively, results in a lack of functional redundancy. This makes its overall performance profile more susceptible to the ablation of individual attention heads.

As each head in Gemma accounts for a significantly larger proportion of the model’s total functional capacity, the ablation of a single head creates a more severe information bottleneck than in denser models. This indicates that while the functional redundancy of high- $\langle \text{BOS} \rangle$  heads is a universal trait, the impact of removing critical low- $\langle \text{BOS} \rangle$  heads is inversely proportional to the total head density of the architecture.

**Layer-wise Concentration in Deeper Blocks** To understand the structural distribution of redundancy, we analyze the mean performance impact of heads within each layer. As shown in Figure 3,  $\langle \text{BOS} \rangle$  sink scores exhibit a clear positional bias, with a significant concentration of high scores in the higher layers of the architectures.

In the final blocks of these architectures, the

surge in average <BOS> scores directly correlates with a high degree of mean functional redundancy per head. Specifically, the average performance drop caused by ablating a single head in these deeper, high-<BOS> layers is negligible, with the models consistently maintaining their baseline accuracy.

Interestingly, we observe model-specific patterns in the initial layers (e.g, Layer 0 to 5). In Qwen3-4B and Gemma-3-4B, single-head ablations have a negligible impact on accuracy despite notably low <BOS> sink scores. Conversely, Llama-3.1-8B exhibits a sharp increase in <BOS> sink scores in its earliest layers, often accompanied by a decrease in accuracy. This suggests that while high <BOS> scores generally signal redundancy, the specific role of the <BOS> token in the very beginning of the network may differ significantly depending on the model’s architecture or training process.

## 5 Mechanistic Evidence: Sink Heads as Attention Dumping Grounds

**Operational Characteristics** A <BOS> sink head is defined by two primary traits: (i) a disproportionately high <BOS> sink score  $S_{\text{BOS}}^{(l,h)}$ , and (ii) near-zero functional sensitivity under ablation. As illustrated in Figure 2, heads in the high-<BOS> regime across Gemma-3, Llama-3.1, and Qwen3 consistently show negligible impact on MMLU accuracy when removed. This behavior suggests that these heads do not transform or convey critical semantic information but instead serve as a stable numerical outlet within the attention mechanism.

**The Softmax Bottleneck and Redundancy** This phenomenon stems from the Softmax constraint, which forces models to allocate attention even in the absence of semantically relevant tokens (Xiao et al., 2024). We propose that as models process deeper layers, specific heads increasingly converge to the <BOS> token as a non-semantic *dumping ground*—a transition qualitatively characterized through the attention signatures in Appendix A. By anchoring to this constant feature, these higher-layer heads maintain a nearly invariant contribution to the residual stream, effectively shifting from semantic processing to purely structural maintenance.

**Layer-wise Localization of Redundancy** The concentration of these dumping grounds in deeper blocks is driven by the stabilization of representations in higher layers. As the model reaches a con-

sensus on the input’s meaning, additional attention heads become functionally redundant, repurposed as numerical outlets to satisfy the softmax-induced requirement. This localized redundancy explains the minimal performance impact of pruning deeper layers. Consequently, high <BOS> sink scores offer a robust proxy for identifying this layer-specific redundancy, providing a clear empirical basis for efficient structural pruning in the model’s final stages.

## 6 <BOS> Sink-based Structured Pruning

Based on the evidence of <BOS> sink heads as redundancy repositories, we introduce a structured pruning strategy that employs the <BOS> sink score to identify and eliminate redundant components.

**Pruning Criterion** We rank architectural components by their <BOS> sink scores and prune those with the highest values. Specifically, attention heads are selected based on  $S_{\text{BOS}}^{(l,h)}$ , while entire transformer blocks are pruned using the layer-wise aggregate  $S_{\text{BOS}}^{(l)}$  as defined in Equation 2. To ensure representation stability, the first and last transformer blocks of each model are excluded from the pruning process.

**Implementation (Head Ablation)** For head-wise pruning, the ablation is implemented by zeroing out the weights in the output projection matrix ( $W_O$ ) corresponding to the identified redundant heads. Specifically, for a target head  $h$  in layer  $l$ , we set its associated weight slice  $W_O^{(l,h)} \in \mathbb{R}^{d_{\text{head}} \times d_{\text{model}}}$  to zero:

$$W_O^{(l,h)} \leftarrow \mathbf{0} \quad (4)$$

This operation ensures that the information processed by head  $h$  is nullified before it can be integrated into the residual stream, effectively removing its functional influence while maintaining the model’s structural integrity.

## 7 Experiments

### 7.1 Experimental Setup

**Models and Benchmarks** We perform evaluations using three LLMs that employ Grouped-Query Attention (GQA): Gemma-3-4B (Team et al., 2025), Llama-3.1-8B (Grattafiori et al., 2024), and Qwen3-4B (Yang et al., 2025a). All experiments are conducted with a maximum sequence length of 4,096 tokens.

Model	Strategy	Pruning Ratio	Wikitext-2 ↓	ARC-c	ARC-e	BoolQ	HellaS.	MMLU	OBQA	PIQA	WG	Avg.
Gemma-3-4B	Dense	0	10.21	0.533	0.816	0.791	0.580	0.597	0.352	0.788	0.725	0.648
	Mag-sp	0.125	17.98	0.421	0.754	0.624	0.451	0.442	0.324	0.767	0.559	0.543
	Wanda-sp		13.53	0.470	0.786	0.724	0.508	0.540	0.318	0.771	0.635	0.594
	Ours (<BOS>)		11.27	0.522	0.813	0.770	0.571	0.594	0.348	0.788	0.718	0.641
Llama-3.1-8B	Dense	0	7.71	0.550	0.822	0.829	0.618	0.653	0.336	0.791	0.781	0.673
	Mag-sp	0.250	315.21	0.225	0.612	0.414	0.321	0.229	0.220	0.695	0.507	0.403
	Wanda-sp		10.75	0.410	0.796	0.760	0.487	0.344	0.330	0.779	0.668	0.572
	Ours (<BOS>)		20.55	0.521	0.810	0.787	0.589	0.524	0.316	0.778	0.722	0.631
Qwen3-4B	Dense	0	17.31	0.584	0.804	0.851	0.532	0.701	0.294	0.753	0.672	0.649
	Mag-sp	0.125	30.91	0.386	0.662	0.569	0.401	0.459	0.248	0.708	0.585	0.502
	Wanda-sp		18.48	0.542	0.760	0.804	0.513	0.653	0.306	0.734	0.637	0.618
	Ours (<BOS>)		19.87	0.568	0.794	0.817	0.534	0.690	0.302	0.755	0.685	0.643

Table 1: Performance comparison of component-level pruning strategies. Wikitext-2 perplexity and downstream accuracy across Llama-3.1-8B, Qwen3-4B, and Gemma-3-4B. Our <BOS>-based strategy consistently outperforms Mag-SP and Wanda-SP, closely matching dense baseline performance.

To assess model performance, we utilize the lm-evaluation-harness<sup>1</sup> (Sutawika et al., 2023) framework across various benchmarks. Specifically, we evaluate WikiText-2 (Merity et al., 2017), ARC-Easy (Clark et al., 2018), BoolQ (Clark et al., 2019a), OpenbookQA (Mihaylov et al., 2018), and PIQA (Bisk et al., 2020) in zero-shot. For few-shot evaluations, we employ 5-shot for Winogrande (Sakaguchi et al., 2019) and MMLU (Hendrycks et al., 2021), 10-shot for Hellaswag (Zellers et al., 2019), and 25-shot for ARC-Challenge (Clark et al., 2018).

**Baselines and Implementation** We compare our approach against several pruning baselines: Wanda-SP (An et al., 2024), Mag-SP (An et al., 2024), and ShortGPT (Men et al., 2025). For layer-level pruning experiments, we additionally evaluate two naive positional strategies: Bottom-Up, which removes transformer blocks sequentially starting from the initial layer, and Top-Down, which starts from the final layer. These positional baselines verify whether the observed redundancy is tied to specific functional metrics or is simply a consequence of a layer’s position within the architecture. In all experiments, the first and last layers of each model were preserved to maintain stable initial feature extraction and final output representation.

Although the official implementations of Wanda-SP and Mag-SP are available via the FLAP (An et al., 2024) repository<sup>2</sup>, they do not natively support models with Grouped-Query Attention (GQA) architectures. Consequently, we extended their core logic to accommodate GQA structures and

reimplemented all baseline methods for our evaluation.

## 7.2 Pruning Results

**Component-level Pruning** Table 1 summarizes the performance of various component-level pruning strategies across Llama-3.1-8B, Qwen3-4B, and Gemma-3-4B. Our proposed <BOS>-based pruning consistently demonstrates superior performance retention across all evaluated architectures and benchmarks.

For Gemma-3-4B and Qwen3-4B, at a 12.5% pruning ratio, the <BOS>-based strategy maintains an average accuracy of 0.641 and 0.643, respectively, which is remarkably close to their dense baselines (0.648 and 0.649). In contrast, Wanda-sp and Mag-sp suffer significant degradations, with their average performance dropping by 10 to 15 percentage points. Even at a more aggressive pruning ratio of 25.0% for Llama-3.1-8B, our method preserves a high level of functional capability with an average accuracy of 0.631, significantly outperforming Wanda-sp (0.572) and Mag-sp (0.403). Detailed performance trajectories across varying pruning ratios can be found in Appendix B.

Notably, while Wanda-sp shows lower perplexity on Wikitext-2 for Llama-3.1-8B (10.75 vs. 20.55), this does not translate into downstream task accuracy, where our <BOS>-based method maintains much higher scores across reasoning benchmarks such as ARC and MMLU. This discrepancy suggests that <BOS> sink scores serve as a more reliable proxy for identifying components critical to complex inference than simple magnitude or activation metrics. These results empirically validate our ablation studies, confirming that components

<sup>1</sup><https://github.com/EleutherAI/lm-evaluation-harness>

<sup>2</sup><https://github.com/CASIA-LMC-Lab/FLAP>

Model	Strategy	Pruning Ratio	Wikitext-2 ↓	ARC-c	ARC-e	BoolQ	HellaS.	MMLU	OBQA	PIQA	WG	Avg.
Gemma-3-4B	Dense	0	10.21	0.533	0.816	0.791	0.580	0.597	0.352	0.788	0.725	0.648
	Bottom Up	0.125	50643.64	0.206	0.314	0.466	0.260	0.241	0.146	0.549	0.488	0.334
	Top Down		45.68	0.379	0.629	0.254	0.427	0.178	0.274	0.717	0.657	0.439
	ShortGPT		20.82	0.307	0.673	0.412	0.431	0.283	0.254	0.743	0.549	0.456
Llama-3.1-8B	Dense	0	7.71	0.550	0.822	0.829	0.618	0.653	0.336	0.791	0.781	0.673
	Bottom Up	0.250	129826.91	0.206	0.270	0.456	0.260	0.228	0.132	0.536	0.493	0.323
	Top Down		<b>1202.52</b>	<b>0.270</b>	0.362	<b>0.622</b>	0.249	<b>0.523</b>	<b>0.220</b>	0.578	<b>0.582</b>	<b>0.426</b>
	ShortGPT		7211.05	0.269	0.436	0.375	0.271	0.342	0.194	0.614	0.542	0.380
Qwen3-4B	Dense	0	17.31	0.584	0.804	0.851	0.532	0.701	0.294	0.753	0.672	0.649
	Bottom Up	0.125	120.72	0.260	0.513	0.572	0.301	0.293	0.178	0.586	0.499	0.400
	Top Down		72.55	0.408	0.614	0.717	0.392	<b>0.682</b>	0.236	0.648	0.633	0.541
	ShortGPT		<b>41.62</b>	<b>0.460</b>	0.662	0.564	<b>0.450</b>	0.673	0.240	<b>0.680</b>	0.623	0.544
Ours (<BOS>)	Dense	0.125	49.89	0.451	<b>0.666</b>	<b>0.826</b>	0.441	0.611	<b>0.252</b>	0.674	<b>0.642</b>	<b>0.570</b>

Table 2: Performance comparison of layer-level pruning strategies. Wikitext-2 perplexity and downstream accuracy across Llama-3.1-8B, Qwen3-4B, and Gemma-3-4B. Our <BOS> -based strategy frequently surpasses positional (Bottom-Up, Top-Down) and ShortGPT baselines, validating <BOS> sink scores as a reliable indicator of transformer block redundancy.

with high <BOS> scores are functionally redundant and can be removed with minimal impact on the model’s core task-solving capabilities.

**Layer-level Pruning** Table 2 presents the results of pruning entire transformer blocks based on different strategies. While component-level pruning focuses on individual heads, layer-level pruning removes both attention and FFN sub-layers simultaneously.

Our <BOS>-based strategy demonstrates significant robustness, particularly for Gemma-3-4B and Qwen3-4B. In Gemma-3-4B, the <BOS> strategy achieves an average accuracy of 0.589, substantially outperforming the next best baseline, ShortGPT (0.456), and significantly avoiding the catastrophic failure observed in the Bottom-Up approach. For Qwen3-4B, the BOS strategy similarly leads with an average accuracy of 0.570, compared to 0.544 for ShortGPT and 0.541 for Top-Down.

In the case of Llama-3.1-8B at a higher pruning ratio of 25.0%, our method remains competitive with an average accuracy of 0.390, outperforming ShortGPT (0.380) and Bottom-Up (0.323), although the Top-Down approach shows higher retention in certain tasks (0.426). These empirical results across diverse architectures suggest that layers characterized by a high concentration of <BOS> sink scores are functionally less critical, allowing for aggressive structural pruning with minimized performance impact.

## 8 Analysis: Consistency Across Context Lengths

To further validate the reliability of <BOS> sink scores as a pruning metric, we investigate their stability across varying input sequence lengths  $T$ .

**Scaling and Structural Normalization** By definition, the <BOS> sink score represents the average of attention weights assigned to the <BOS> token throughout a sequence. Due to the Softmax operation’s normalization—where the sum of attention weights for each query must equal 1—the average attention weight per token naturally scales with  $1/T$ . Consequently, as  $T$  increases, absolute <BOS> sink scores exhibit an inevitable downward trend across all heads. This reduction should be viewed as a structural consequence of the attention mechanism’s normalization rather than a loss of functional importance.

**Differential Stability of Sink Heads** Notably, we observe a clear correlation between a head’s average <BOS> sink score  $\mu$  and its robustness to increasing sequence lengths. As illustrated in Figure 4, the rate of decline in attention scores is inversely related to the magnitude of  $\mu$ : while the average score for all heads drops sharply, heads with  $\mu \geq 0.6$  show more tempered decreases, and those with  $\mu \geq 0.8$  exhibit the most gradual downward trajectories. This differential stability indicates that higher-scoring <BOS> sink heads appear to partially mitigate the  $1/T$  scaling effect, maintaining a disproportionately high focus on the <BOS> token even as the total attention budget is distributed over an

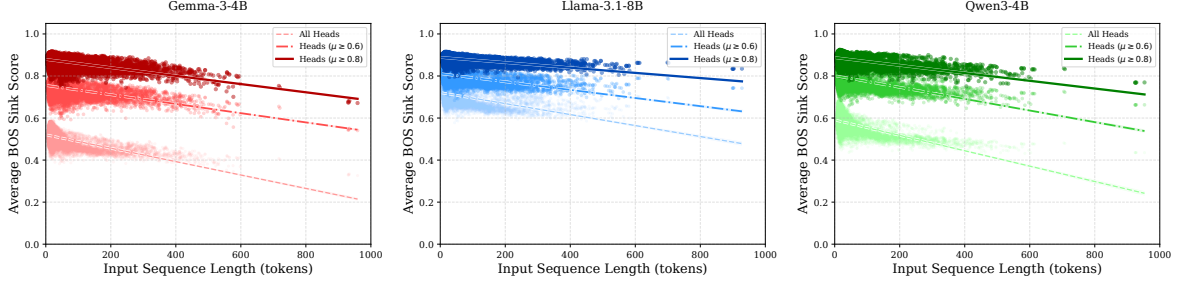


Figure 4: Scaling of average  $\langle \text{BOS} \rangle$  sink scores with sequence length  $T$ . Each point represents the mean  $\langle \text{BOS} \rangle$  sink score across all attention heads for a specific input. Dashed, dash-dotted, and solid lines denote linear regressions for all heads, heads with  $\mu \geq 0.6$ , and  $\mu \geq 0.8$ , respectively. Despite the  $1/T$  softmax scaling effect, specialized sink heads (higher  $\mu$ ) exhibit markedly more gradual slopes, indicating greater robustness and more consistent  $\langle \text{BOS} \rangle$  focus as context length increases.

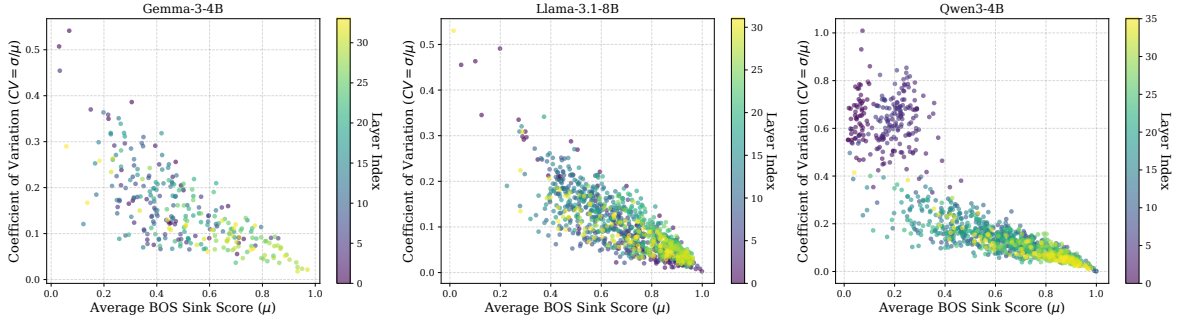


Figure 5: Relationship between the mean  $\langle \text{BOS} \rangle$  sink score ( $\mu$ ) and the Coefficient of Variation ( $CV$ ). Each dot represents an individual attention head, color-coded by its layer index. A clear inverse correlation is observed: heads with higher  $\mu$  exhibit lower  $CV$  values. Notably, these consistent  $\langle \text{BOS} \rangle$  sink heads are primarily situated in the higher layers of the model, highlighting that functional stability and structural redundancy are deeply intertwined with the model’s depth.

increasingly large number of tokens.

**Positional Bias and Convergence** Furthermore, our analysis reveals a strong positional bias in the emergence and stability of these heads. To quantify this, we utilize the Coefficient of Variation ( $CV = \sigma/\mu$ ), where  $\sigma$  and  $\mu$  represent the standard deviation and mean of the  $\langle \text{BOS} \rangle$  sink scores across different sequence lengths. As shown in Figure 5, a clear inverse correlation exists between  $\mu$  and  $CV$ . Crucially, heads with high  $\mu$  and near-zero  $CV$  are predominantly concentrated in the deeper layers of the architecture (indicated by the yellow and green hues). This suggests that as the model’s layers deepen, certain heads converge into stable  $\langle \text{BOS} \rangle$  sinks that maintain consistent attention patterns regardless of the input sequence length.

## 9 Conclusion

In this study, we established the  $\langle \text{BOS} \rangle$  sink phenomenon as a primary driver of functional redundancy in LLMs, revealing a strong correlation be-

tween high  $\langle \text{BOS} \rangle$  sink scores and negligible predictive contribution. Our findings provide a systematic explanation for the high redundancy observed in deeper layers, where specialized heads act as stable repositories for unnecessary attention weights, effectively functioning as internal *dumping grounds*. By bridging the gap between internal attention patterns and layer-wise sensitivity, we demonstrated that structural attention properties can serve as a more efficient and direct alternative to traditional weight-based metrics for hardware-friendly model compression. Experiments across Gemma-3, Llama-3.1, and Qwen3 confirm that our straightforward  $\langle \text{BOS} \rangle$ -based pruning matches or exceeds the efficacy of established methods like Wanda-SP and Mag-SP.

Future work will focus on validating the  $\langle \text{BOS} \rangle$  sink phenomenon across even larger-scale models and a broader range of downstream tasks to ensure its cross-domain stability. Furthermore, we aim to investigate whether similar attention-anchoring mechanisms exist in other Transformer-based ar-

chitectures beyond text, such as Vision-Language Models (VLMs). Additionally, investigating the developmental dynamics of these sinks during the pre-training phase may offer deeper insights into how models establish representational stability through structural redundancy.

## Limitations

Despite the robust findings presented in this study, several limitations remain.

First, while we established a strong correlation between high  $\langle BOS \rangle$  sink scores and functional redundancy, our work is primarily based on empirical observations. We demonstrated that these specialized heads predominantly emerge and concentrate in the deeper layers of the architecture, yet we do not provide a formal theoretical derivation for the underlying cause of this positional concentration.

Second, although we validated the efficacy of our BOS-based pruning strategy across diverse GQA-based architectures—specifically Gemma-3-4B, Llama-3.1-8B, and Qwen3-4B—the scope of this study is limited to models of specific scales. Further research is required to verify whether these attention patterns and redundancy characteristics generalize to ultra-large scale models.

## Ethical Considerations

**Fairness and Potential Bias** The pruning process, by removing model parameters, carries the risk of inadvertently amplifying biases toward specific demographic groups inherent in the training data. While our study demonstrates robust performance retention on general reasoning benchmarks such as MMLU and ARC, the specific impact on social bias and toxicity remains to be fully characterized. Consequently, we strongly advise conducting a comprehensive evaluation to detect any discriminatory behaviors against marginalized communities before deploying the pruned models in production environments.

**Use of AI Assistants** In accordance with the ACL Policy on AI Assistance, we acknowledge the use of Gemini 3 Pro<sup>3</sup> to assist with code debugging and improving the readability and grammar of this manuscript. The final content and responsibility for the work rest solely with the authors.

## References

Yongqi An, Xu Zhao, Tao Yu, Ming Tang, and Jinqiao Wang. 2024. **Fluctuation-based adaptive structured pruning for large language models**. In *Thirty-Eighth AAAI Conference on Artificial Intelligence, AAAI 2024, Thirty-Sixth Conference on Innovative Applications of Artificial Intelligence, IAAI 2024, Fourteenth Symposium on Educational Advances in Artificial*

---

<sup>3</sup><https://deepmind.google/models/gemini/>

*Intelligence, EAAI 2014, February 20-27, 2014, Vancouver, Canada, pages 10865–10873. AAAI Press.*

Saleh Ashkboos, Maximilian L. Croci, Marcelo Genari Do Nascimento, Torsten Hoefer, and James Hensman. 2024. [Slicecpt: Compress large language models by deleting rows and columns](#). In *The Twelfth International Conference on Learning Representations, ICLR 2024, Vienna, Austria, May 7-11, 2024*. OpenReview.net.

Federico Barbero, Alvaro Arroyo, Xiangming Gu, Christos Perivolaropoulos, Petar Veličković, Razvan Pascanu, and Michael M. Bronstein. 2025. [Why do LLMs attend to the first token?](#) In *Second Conference on Language Modeling*.

Yonatan Bisk, Rowan Zellers, Ronan Le Bras, Jianfeng Gao, and Yejin Choi. 2020. [PIQA: reasoning about physical commonsense in natural language](#). In *The Thirty-Fourth AAAI Conference on Artificial Intelligence, AAAI 2020, The Thirty-Second Innovative Applications of Artificial Intelligence Conference, IAAI 2020, The Tenth AAAI Symposium on Educational Advances in Artificial Intelligence, EAAI 2020, New York, NY, USA, February 7-12, 2020*, pages 7432–7439. AAAI Press.

Tom Brown, Benjamin Mann, Nick Ryder, Melanie Subbiah, Jared D Kaplan, Prafulla Dhariwal, Arvind Neelakantan, Pranav Shyam, Girish Sastry, Amanda Askell, and 1 others. 2020. Language models are few-shot learners. *Advances in neural information processing systems*, 33:1877–1901.

Christopher Clark, Kenton Lee, Ming-Wei Chang, Tom Kwiatkowski, Michael Collins, and Kristina Toutanova. 2019a. [BoolQ: Exploring the surprising difficulty of natural yes/no questions](#). In *Proceedings of the 2019 Conference of the North American Chapter of the Association for Computational Linguistics: Human Language Technologies, Volume 1 (Long and Short Papers)*, pages 2924–2936, Minneapolis, Minnesota. Association for Computational Linguistics.

Kevin Clark, Urvashi Khandelwal, Omer Levy, and Christopher D. Manning. 2019b. [What does BERT look at? an analysis of BERT’s attention](#). In *Proceedings of the 2019 ACL Workshop BlackboxNLP: Analyzing and Interpreting Neural Networks for NLP*, pages 276–286, Florence, Italy. Association for Computational Linguistics.

Peter Clark, Isaac Cowhey, Oren Etzioni, Tushar Khot, Ashish Sabharwal, Carissa Schoenick, and Oyvind Tafjord. 2018. Think you have solved question answering? try arc, the ai2 reasoning challenge. *ArXiv*, abs/1803.05457.

Siqi Fan, Xin Jiang, Xiang Li, Xuying Meng, Peng Han, Shuo Shang, Aixin Sun, and Yequan Wang. 2025. [Not all layers of llms are necessary during inference](#). In *Proceedings of the Thirty-Fourth International Joint Conference on Artificial Intelligence, IJCAI 2025, Montreal, Canada, August 16-22, 2025*, pages 5083–5091. ijcai.org.

Elias Frantar and Dan Alistarh. 2023. Sparsegpt: Massive language models can be accurately pruned in one-shot. In *International conference on machine learning*, pages 10323–10337. PMLR.

Aaron Grattafiori, Abhimanyu Dubey, Abhinav Jauhri, Abhinav Pandey, Abhishek Kadian, Ahmad Al-Dahle, Aiesha Letman, Akhil Mathur, Alan Schelten, Alex Vaughan, Amy Yang, Angela Fan, Anirudh Goyal, Anthony Hartshorn, Aobo Yang, Archi Mitra, Archie Sravankumar, Artem Korenev, Arthur Hinsvark, and 542 others. 2024. [The llama 3 herd of models](#). *Preprint*, arXiv:2407.21783.

Andrey Gromov, Kushal Tirumala, Hassan Shapourian, Paolo Glorioso, and Daniel A. Roberts. 2025. [The unreasonable ineffectiveness of the deeper layers](#). In *The Thirteenth International Conference on Learning Representations, ICLR 2025, Singapore, April 24-28, 2025*. OpenReview.net.

Xiangming Gu, Tianyu Pang, Chao Du, Qian Liu, Fengzhuo Zhang, Cunxiao Du, Ye Wang, and Min Lin. 2025. [When attention sink emerges in language models: An empirical view](#). In *The Thirteenth International Conference on Learning Representations, ICLR 2025, Singapore, April 24-28, 2025*. OpenReview.net.

Song Han, Jeff Pool, John Tran, and William Dally. 2015. Learning both weights and connections for efficient neural network. *Advances in neural information processing systems*, 28.

Shuai He, Guoheng Sun, Zheyu Shen, and Ang Li. 2024. What matters in transformers? not all attention is needed. *arXiv preprint arXiv:2406.15786*.

Dan Hendrycks, Collin Burns, Steven Basart, Andy Zou, Mantas Mazeika, Dawn Song, and Jacob Steinhardt. 2021. [Measuring massive multitask language understanding](#). In *International Conference on Learning Representations*.

Torsten Hoefer, Dan Alistarh, Tal Ben-Nun, Nikoli Dryden, and Alexandra Peste. 2021. Sparsity in deep learning: Pruning and growth for efficient inference and training in neural networks. *Journal of Machine Learning Research*, 22(241):1–124.

Prakhar Kaushik, Shravan Chaudhari, Ankit Vaidya, Rama Chellappa, and Alan Yuille. 2025. The universal weight subspace hypothesis. *arXiv preprint arXiv:2512.05117*.

Songtao Liu and Peng Liu. 2025. High-layer attention pruning with rescaling. *arXiv preprint arXiv:2507.01900*.

Xinyin Ma, Gongfan Fang, and Xinchao Wang. 2023. Llm-pruner: On the structural pruning of large language models. *Advances in neural information processing systems*, 36:21702–21720.

Xin Men, Mingyu Xu, Qingyu Zhang, Qianhao Yuan, Bingning Wang, Hongyu Lin, Yaojie Lu, Xianpei Han, and Weipeng Chen. 2025. Shortgpt: Layers in large language models are more redundant than you expect. In *Findings of the Association for Computational Linguistics: ACL 2025*, pages 20192–20204.

Stephen Merity, Caiming Xiong, James Bradbury, and Richard Socher. 2017. Pointer sentinel mixture models. In *International Conference on Learning Representations*.

Paul Michel, Omer Levy, and Graham Neubig. 2019. Are sixteen heads really better than one? *Advances in neural information processing systems*, 32.

Todor Mihaylov, Peter Clark, Tushar Khot, and Ashish Sabharwal. 2018. Can a suit of armor conduct electricity? a new dataset for open book question answering. In *Proceedings of the 2018 Conference on Empirical Methods in Natural Language Processing*, pages 2381–2391, Brussels, Belgium. Association for Computational Linguistics.

Enrique Queipo-de Llano, Álvaro Arroyo, Federico Barbero, Xiaowen Dong, Michael Bronstein, Yann LeCun, and Ravid Shwartz-Ziv. 2025. Attention sinks and compression valleys in llms are two sides of the same coin. *arXiv preprint arXiv:2510.06477*.

Keisuke Sakaguchi, Ronan Le Bras, Chandra Bhagavatula, and Yejin Choi. 2019. Winogrande: An adversarial winograd schema challenge at scale. *arXiv preprint arXiv:1907.10641*.

Jiwon Song, Kyungseok Oh, Taesu Kim, Hyungjun Kim, Yulhwa Kim, and Jae-Joon Kim. 2024. SLEB: streamlining llms through redundancy verification and elimination of transformer blocks. In *Forty-first International Conference on Machine Learning, ICML 2024, Vienna, Austria, July 21-27, 2024*. OpenReview.net.

Mingjie Sun, Zhuang Liu, Anna Bair, and J. Zico Kolter. 2024. A simple and effective pruning approach for large language models. In *The Twelfth International Conference on Learning Representations, ICLR 2024, Vienna, Austria, May 7-11, 2024*. OpenReview.net.

Lintang Sutawika, Leo Gao, Hailey Schoelkopf, Stella Biderman, Jonathan Tow, Baber Abbasi, ben fattori, Charles Lovering, farzanehnakhaee70, Jason Phang, Anish Thite, Fazz, Aflah, Niklas Muenighoff, Thomas Wang, sdtblk, nopperl, gakada, ttyuntian, and 11 others. 2023. Eleutherai/lm-evaluation-harness: Major refactor.

Gemma Team, Aishwarya Kamath, Johan Ferret, Shreya Pathak, Nino Vieillard, Ramona Merhej, Sarah Perrin, Tatiana Matejovicova, Alexandre Ramé, Morgane Rivière, Louis Rouillard, Thomas Mesnard, Geoffrey Cideron, Jean bastien Grill, Sabela Ramos, Edouard Yvinec, Michelle Casbon, Etienne Pot, Ivo Penchev, and 197 others. 2025. Gemma 3 technical report. *Preprint*, arXiv:2503.19786.

Ashish Vaswani, Noam Shazeer, Niki Parmar, Jakob Uszkoreit, Llion Jones, Aidan N Gomez, Łukasz Kaiser, and Illia Polosukhin. 2017. Attention is all you need. *Advances in neural information processing systems*, 30.

Elena Voita, David Talbot, Fedor Moiseev, Rico Sennrich, and Ivan Titov. 2019. Analyzing multi-head self-attention: Specialized heads do the heavy lifting, the rest can be pruned. In *Proceedings of the 57th Annual Meeting of the Association for Computational Linguistics*, pages 5797–5808, Florence, Italy. Association for Computational Linguistics.

Guangxuan Xiao, Yuandong Tian, Beidi Chen, Song Han, and Mike Lewis. 2024. Efficient streaming language models with attention sinks. In *The Twelfth International Conference on Learning Representations, ICLR 2024, Vienna, Austria, May 7-11, 2024*. OpenReview.net.

An Yang, Anfeng Li, Baosong Yang, Beichen Zhang, Binyuan Hui, Bo Zheng, Bowen Yu, Chang Gao, Chengan Huang, Chenxu Lv, Chujie Zheng, Dayiheng Liu, Fan Zhou, Fei Huang, Feng Hu, Hao Ge, Haoran Wei, Huan Lin, Jialong Tang, and 41 others. 2025a. Qwen3 technical report. *Preprint*, arXiv:2505.09388.

Liangwei Yang, Yuhui Xu, Juntao Tan, Doyen Sahoo, Silvio Savarese, Caiming Xiong, Huan Wang, and Shelby Heinecke. 2025b. Entropy-based block pruning for efficient large language models. *arXiv preprint arXiv:2504.03794*.

Yifan Yang, Kai Zhen, Bhavana Ganesh, Aram Galstyan, Goeric Huybrechts, Markus Müller, Jonas M. Kübler, Rupak Vignesh Swaminathan, Athanasios Mouchtaris, Sravan Babu Bodapati, Nathan Susanj, Zheng Zhang, Jack FitzGerald, and Abhishek Kumar. 2025c. Wanda++: Pruning large language models via regional gradients. In *Findings of the Association for Computational Linguistics: ACL 2025, Vienna, Austria, July 27 - August 1, 2025*, pages 4321–4333. Association for Computational Linguistics.

Yifei Yang, Zouying Cao, and Hai Zhao. 2024. Laco: Large language model pruning via layer collapse. In *Findings of the Association for Computational Linguistics: EMNLP 2024, Miami, Florida, USA, November 12-16, 2024*, pages 6401–6417. Association for Computational Linguistics.

Rowan Zellers, Ari Holtzman, Yonatan Bisk, Ali Farhadi, and Yejin Choi. 2019. Hellaswag: Can a machine really finish your sentence? In *Proceedings of the 57th Conference of the Association for Computational Linguistics, ACL 2019, Florence, Italy, July 28- August 2, 2019, Volume 1: Long Papers*, pages 4791–4800. Association for Computational Linguistics.

Yang Zhang, Yawei Li, Xinpeng Wang, Qianli Shen, Barbara Plank, Bernd Bischl, Mina Rezaei, and Kenji

Kawaguchi. 2024. Finercut: Finer-grained interpretable layer pruning for large language models. *arXiv preprint arXiv:2405.18218*.

Wayne Xin Zhao, Kun Zhou, Junyi Li, Tianyi Tang, Xiaolei Wang, Yupeng Hou, Yingqian Min, Beichen Zhang, Junjie Zhang, Zican Dong, and 1 others. 2023. A survey of large language models. *arXiv preprint arXiv:2303.18223*, 1(2).

Xunyu Zhu, Jian Li, Yong Liu, Can Ma, and Weiping Wang. 2024. [A survey on model compression for large language models](#). *Transactions of the Association for Computational Linguistics*, 12:1556–1577.

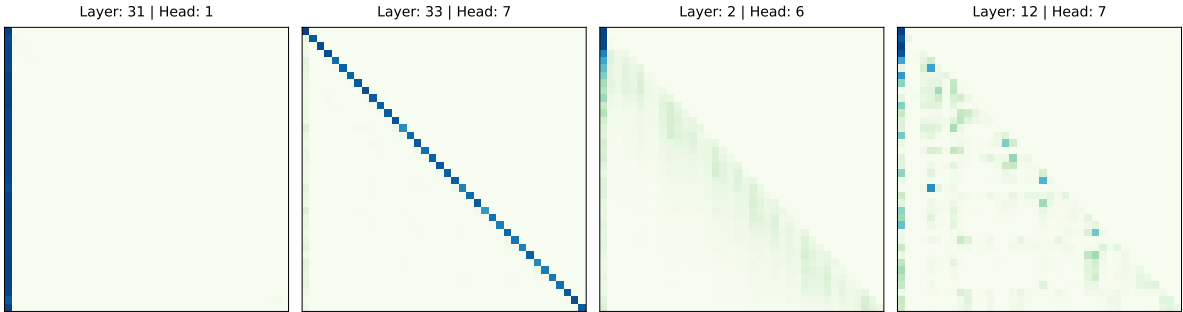


Figure 6: Visualization of four representative attention patterns in Gemma-3-4B during MMLU tasks. From left to right, the maps illustrate: (1) **BOS Sink** showing intense focus on the initial token (Layer 31, Head 1); (2) **Diagonal (Self-Attention)** with weights concentrated strictly on the query token (Layer 33, Head 7); (3) **Uniform** broad attention distribution primarily observed in lower layers (Layer 2, Head 6); and (4) **Random** sparse attention patterns (Layer 12, Head 7).

## A Patterns of Attention

To qualitatively characterize the attention behaviors underlying model redundancy, we visualize the attention maps of Gemma-3-4B during inference. As illustrated in Figure 6, we identify four representative patterns that define the functional landscape of the attention mechanism: BOS Sink, Diagonal, Uniform, and Random. Our qualitative analysis of these signatures yields three primary findings regarding the structural properties of these attention heads.

**Dominance of Non-Transformative Patterns** A significant majority of attention heads exhibit either BOS sink or Diagonal patterns. While BOS sinks are known as repositories for unnecessary attention weights, we hypothesize that Diagonal patterns may serve a similar function. In a residual architecture, a head attending solely to its own position effectively acts as an identity map, contributing no new contextual information to the hidden state and thus remaining functionally redundant.

**Layer-wise Specialization** Uniform patterns, which facilitate broad information mixing, are predominantly concentrated in the lower layers (e.g., Layer 2). This suggests that global contextual integration occurs early in the forward pass, while deeper layers transition toward specialized "dumping grounds" behaviors like BOS or Diagonal sinks.

**Functional Stability** We observed that these attention signatures tend to remain input-invariant. Regardless of changes in the input sequence, individual heads appear to maintain their specific

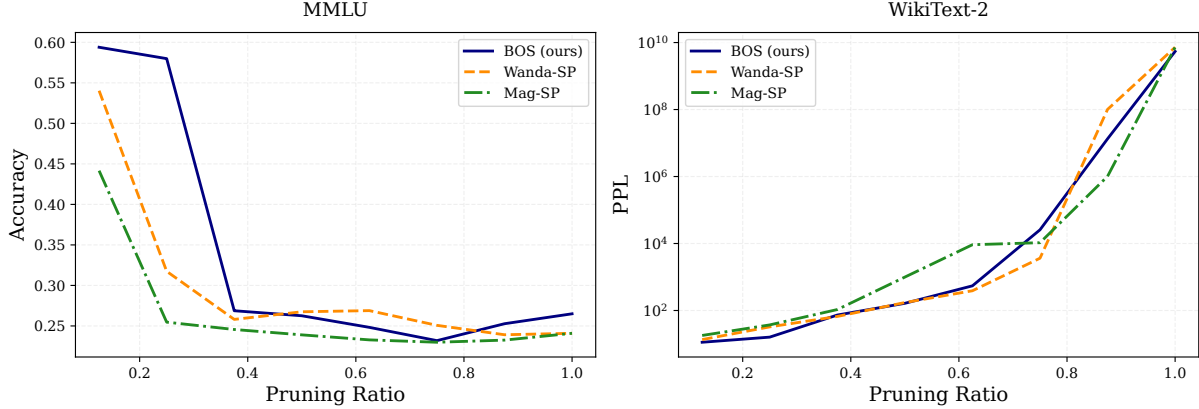
patterns. This stability suggests that attention behaviors could be interpreted as structural traits inherent to the pre-trained architecture, rather than purely dynamic responses to specific semantic content. While these observations provide meaningful insights, a more rigorous validation remains for future work to confirm the extent of this inherent stability.

## B Robustness to Model Pruning

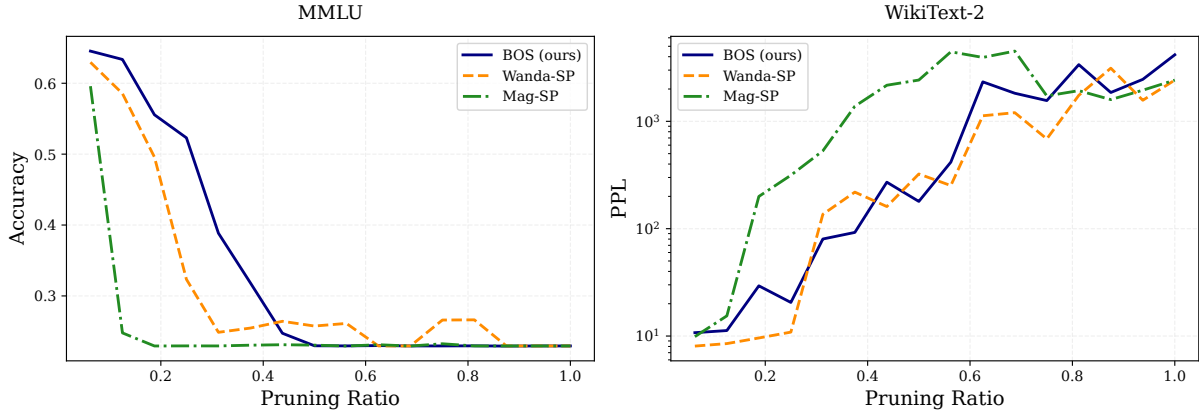
To evaluate the efficacy of our proposed method, we conduct component-level pruning on various LLMs, including Gemma-3-4B, Qwen3-4B, and Llama-3.1-8B, and measure their performance on MMLU (5-shot) and WikiText-2. As illustrated in Figure 7, our method exhibits significantly higher robustness in terms of MMLU accuracy compared to competitive baselines such as Wanda-SP and Mag-SP.

Regarding perplexity, although BOS shows a relatively sharp increase when the pruning ratio exceeds 0.5, it remains highly competitive and comparable to the baselines within the low-to-moderate pruning range (up to 0.5). Since pruning ratios beyond 0.5 often lead to non-functional models in practical deployments, the superior performance of BOS in the practically meaningful regime highlights its effectiveness for real-world model compression.

### Gemma-3-4B



### Llama-3.1-8B



### Qwen3-4B

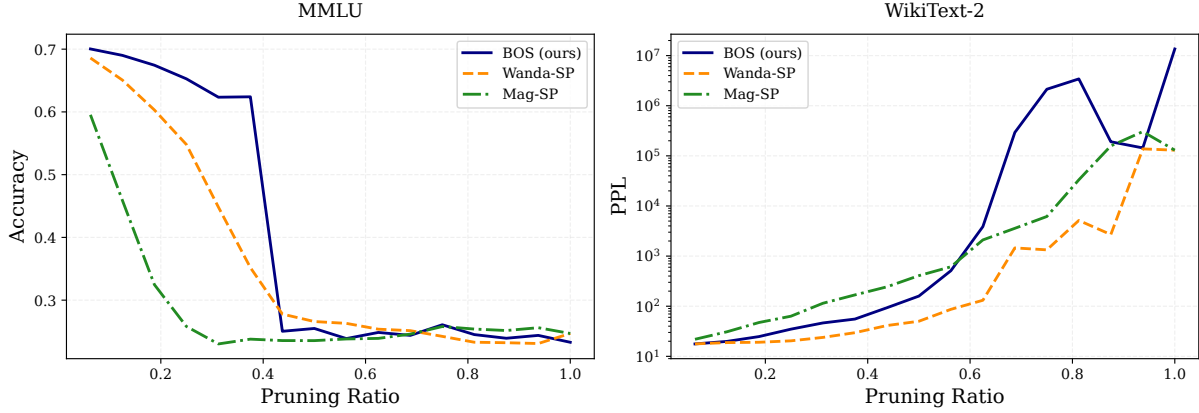


Figure 7: Performance comparison of component-level pruning methods on Gemma-3-4B, Qwen3-4B, and Llama-3.1-8B. We report MMLU 5-shot accuracy and WikiText-2 perplexity as a function of the pruning ratio. Our method, consistently demonstrates superior robustness in accuracy across all models and throughout the entire range of pruning ratios compared to the baselines.

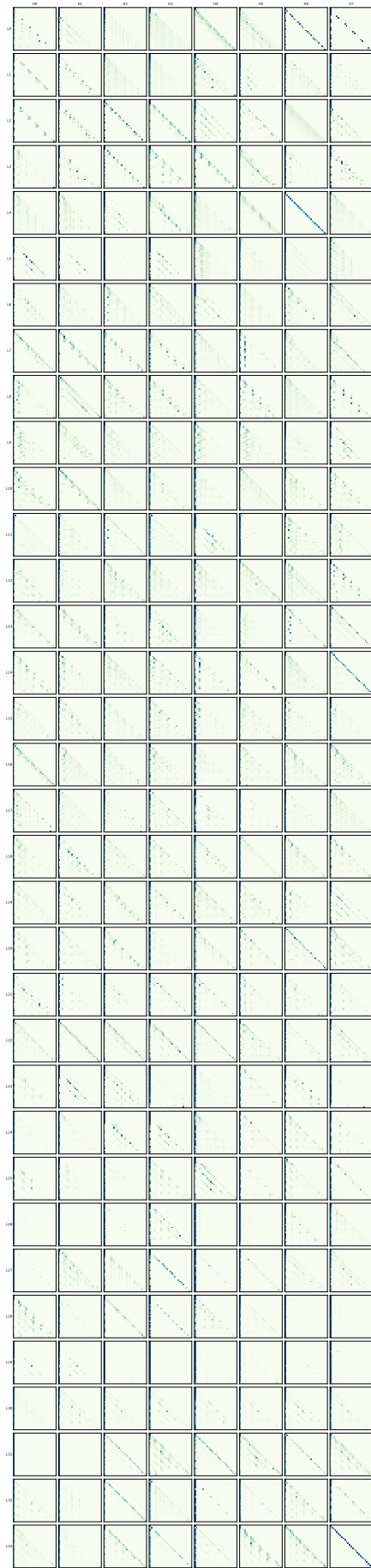


Figure 8: Full Attention Maps for Gemma-3-4B.

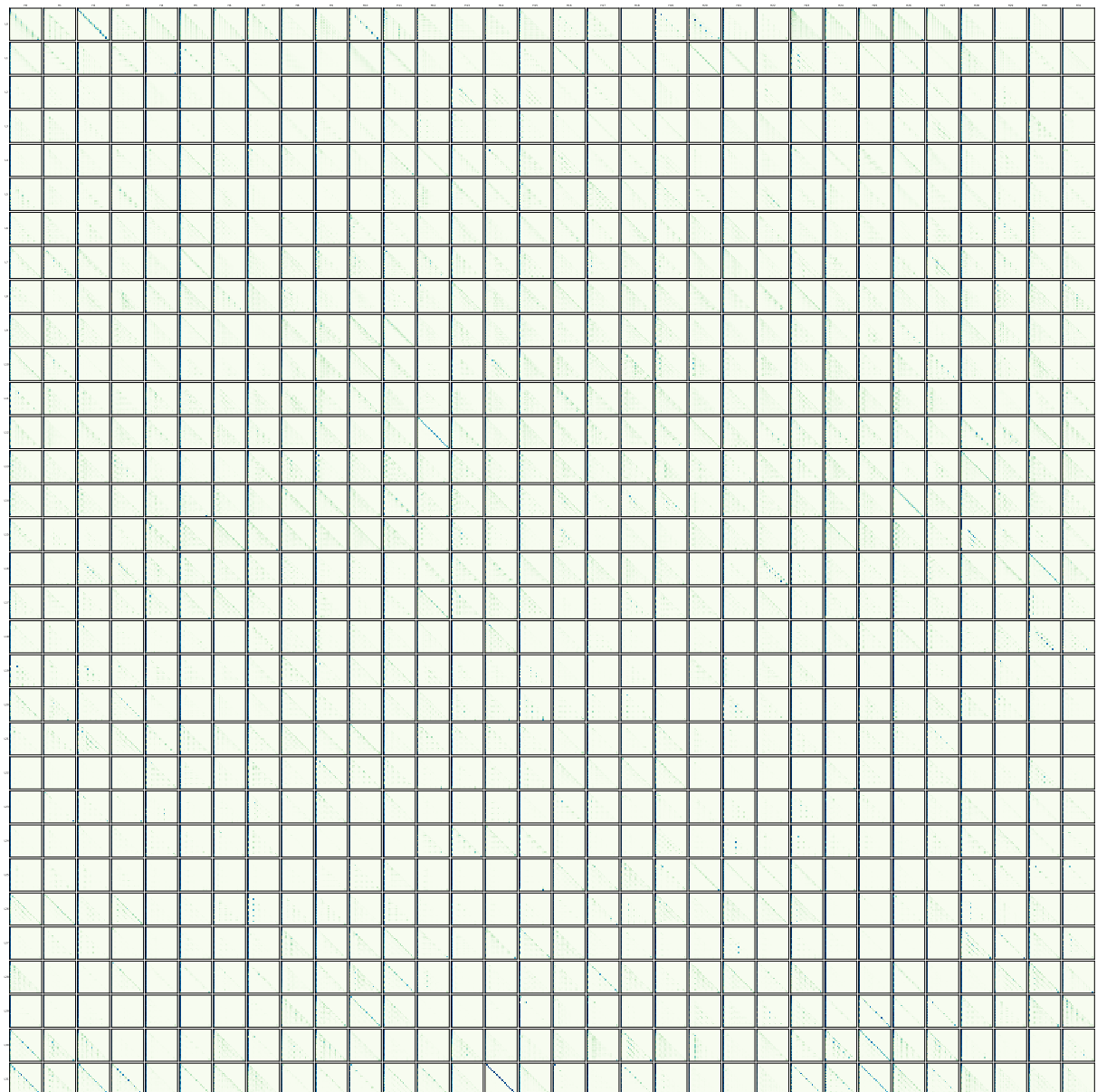


Figure 9: Full Attention Maps for Llama-3.1-8B.

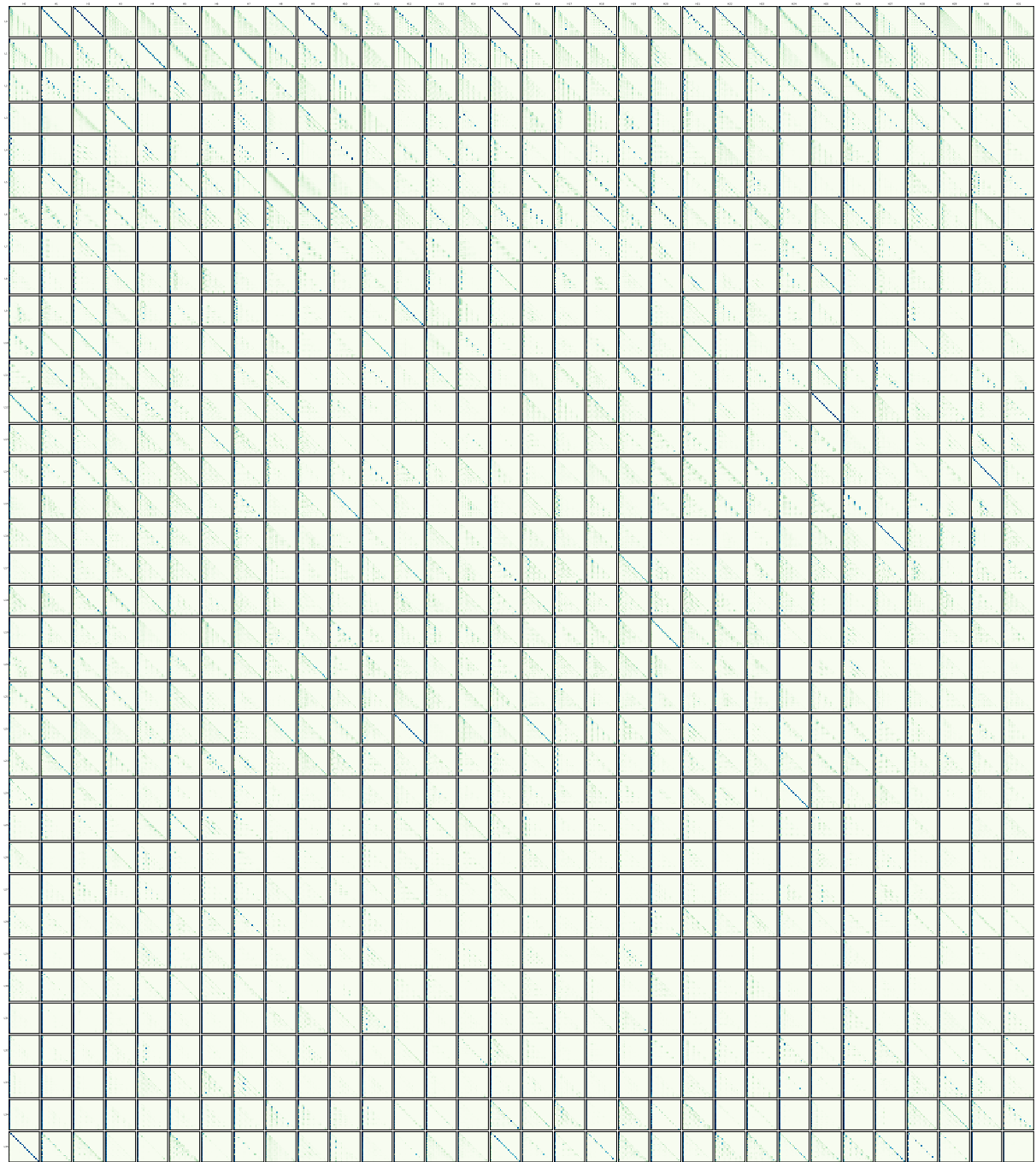


Figure 10: Full Attention Maps for Qwen3-4B.